


Precision CP Symmetry Test and Polarization Analysis in Σ^+ DecaysM. Ablikim *et al.*^{*}
(BESIII Collaboration) (Received 21 March 2025; revised 13 May 2025; accepted 16 September 2025; published 1 October 2025)

A stringent test of CP symmetry in hyperon decays is performed using 1.0×10^{10} J/ψ events and 2.7×10^9 $\psi(3686)$ events collected by the BESIII experiment. The CP asymmetry in the two-body nonleptonic weak decays $\Sigma^+ \rightarrow p\pi^0$ and $\bar{\Sigma}^- \rightarrow \bar{p}\pi^0$ is determined to be $A_{CP} = -0.0118 \pm 0.0083(\text{stat}) \pm 0.0028(\text{syst})$, consistent with CP conservation. The average decay parameter $\langle\alpha_0\rangle = -0.9869 \pm 0.0011(\text{stat}) \pm 0.0016(\text{syst})$ represents the most precise measurement in the baryon sector to date. A model-independent analysis of the hyperon polarization is performed for the first time at J/ψ and $\psi(3686)$ resonances, revealing a clear sign reversal and offering new insight into SU(3) symmetry breaking and baryon internal structure. These results provide the most stringent constraints on CP violation in Σ decays and establish a benchmark for future precision studies.

DOI: [10.1103/ysd5-s2gn](https://doi.org/10.1103/ysd5-s2gn)

Violation of charge conjugation and parity (CP) symmetry is one of the necessary conditions to explain the abundance of matter with respect to antimatter in the Universe [1]. While CP violation has been observed in decays of K , B , and D mesons through the Kobayashi-Maskawa mechanism [2–9], the effects predicted by the standard model (SM) are insufficient to account for the matter-antimatter asymmetry [10], indicating the need for additional CP violation sources beyond the SM (BSM) [11–15].

Since most visible matter consists of baryons, exploring CP violation in the baryon sector is particularly important. Recently, the LHCb Collaboration reported evidence for CP violation in Λ_b^0 decay into $\Lambda K^+ K^-$ [16] and the first observation of CP violation in Λ_b^0 four-body decay [17]. However, these results pertain to heavy-flavor baryons and involve complex multibody final states. In contrast, hyperon decays, dominated by light quarks and two-body decay modes, offer a complementary and theoretically cleaner avenue for probing CP violation. Unlike branching-fraction asymmetries used in heavy baryon CP studies, nonleptonic two-body hyperon decays are characterized by decay asymmetry parameters α_h and $\bar{\alpha}_h$ for hyperons and antihyperons, respectively [18]. CP symmetry can be tested by the CP -odd observable $A_{CP} = (\alpha_h + \bar{\alpha}_h)/(\alpha_h - \bar{\alpha}_h)$, where a value significantly deviating from zero would indicate CP violation [19–22]. Predictions for the

$A_{CP}(\Sigma^+ \rightarrow p\pi^0)$ asymmetry in the SM range from -3.2×10^{-7} [23] to 3.6×10^{-6} [24]. Several BSM theories predict an order of magnitude larger values, for example, -3.2×10^{-5} with the Weinberg-Higgs model and -2.9×10^{-5} with the left-right-symmetric model [23]. The BESIII Collaboration has previously reported the first measurement, based on a subset of its J/ψ and $\psi(3686)$ data [25,26], yielding $A_{CP}(\Sigma^+ \rightarrow p\pi^0) = 0.004 \pm 0.037 \pm 0.010$, consistent with CP conservation. The average decay asymmetry parameter was also determined to be $-0.994 \pm 0.004 \pm 0.002$ [22]. Beyond the role of parameter α_h in CP violation test, it also provides valuable insight into hadronic structure. Achieving improved precision in hyperon CP violation is crucial for testing BSM theories and understanding the matter-antimatter imbalance in the Universe.

—In addition to hyperon decay observables, the hyperon pair production carries essential information about the underlying dynamics, particularly the internal structure of hyperons. The production is characterized by the angular distribution parameter α_ψ and the hyperon polarization \vec{P}_h . The Σ hyperon exhibits distinct behaviors compared to other hyperons such as Λ and Ξ . In particular, the sign of α_ψ is found to be opposite at the J/ψ and $\psi(3686)$ resonances, in contrast to the same-sign behavior observed in other hyperons, which could be explained with SU(3) symmetry-breaking model [27]. In $\Sigma^+ \bar{\Sigma}^-$ pair production, a polarization sign flip is also observed, which again differs from the behavior seen in Λ and Ξ hyperons. Notably, SU(3) symmetry breaking alone does not provide a satisfactory explanation for this phenomenon. Alternative interpretations involving diquark correlations [28,29] and hadronic loop corrections have been proposed. Therefore, more precise measurements of hyperon polarization are needed to elucidate hyperon dynamics and structure.

^{*}Full author list given at the end of the Letter.

Published by the American Physical Society under the terms of the [Creative Commons Attribution 4.0 International](https://creativecommons.org/licenses/by/4.0/) license. Further distribution of this work must maintain attribution to the author(s) and the published article's title, journal citation, and DOI. Funded by SCOAP³.

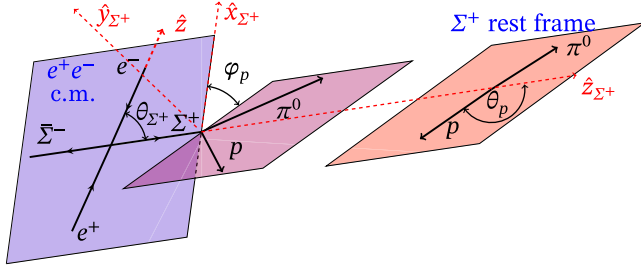


FIG. 1. The helicity frame definition for the decay processes $\Psi \rightarrow \Sigma^+ \bar{\Sigma}^-$, $\Sigma^+ \rightarrow p \pi^0$, and $\bar{\Sigma}^- \rightarrow \bar{p} \pi^0$ in the center-of-mass (c.m.) system of the $e^+ e^-$ collision. The helicity angles are defined with respect to the direction of the outgoing hyperon in the c.m. frame, where \hat{z}_{Σ^+} is defined along the Σ^+ momentum direction in the c.m. of the $e^+ e^-$ collision.

In this Letter, we present a stringent test of CP symmetry in $\Sigma^+ \rightarrow p \pi^0$ and $\bar{\Sigma}^- \rightarrow \bar{p} \pi^0$ decays, based on 1.0×10^{10} J/ψ [30] and 2.7×10^9 $\psi(3686)$ events [31] collected by the BESIII experiment, which are 7.7 and 6.1 times larger, respectively, than those used previously. Exploiting the quantum entanglement of $\Sigma^+ \bar{\Sigma}^-$ pairs produced in J/ψ and $\psi(3686)$ decays, we achieve the most sensitive test of CP violation in Σ decay to date. Furthermore, we perform the first model-independent measurement of the polarization ratios between J/ψ and $\psi(3686)$, providing critical new insights into hyperon structure and strong interaction dynamics.

To extract the decay and production parameters with high precision, a theoretical framework is established to describe the joint angular distribution of the $\Sigma^+ \bar{\Sigma}^-$ system [32–35]. In this framework, the full process $e^+ e^- \rightarrow \Psi \rightarrow \Sigma^+ \bar{\Sigma}^- \rightarrow p \pi^0 \bar{p} \pi^0$ can be characterized by the helicity angles of the final-state particles, an angular-distribution parameter α_Ψ , a relative phase $\Delta\Phi$, and two decay asymmetry parameters. As seen from the basis vector definitions in Fig. 1, θ_{Σ^+} is the angle between the Σ^+ momentum and the electron-beam direction, and θ_p and ϕ_p are the polar and azimuthal angles of the p momentum direction in the Σ^+ rest frame. The joint angular distribution $\mathcal{W}(\xi)$ [32,35,36] of the $e^+ e^- \rightarrow \Psi \rightarrow \Sigma^+ \bar{\Sigma}^-$, $\Sigma^+ \rightarrow p \pi^0$, and $\bar{\Sigma}^- \rightarrow \bar{p} \pi^0$ processes is given by

$$\begin{aligned} \mathcal{W}(\xi) = & T_0(\xi) + \alpha_\Psi T_5(\xi) \\ & + \alpha_0 \bar{\alpha}_0 \left(T_1(\xi) + \sqrt{1 - \alpha_\Psi^2} \cos(\Delta\Phi) T_2(\xi) \right. \\ & \left. + \alpha_\Psi T_6(\xi) \right) \\ & + \sqrt{1 - \alpha_\Psi^2} \sin(\Delta\Phi) (\alpha_0 T_3(\xi) + \bar{\alpha}_0 T_4(\xi)), \quad (1) \end{aligned}$$

where Ψ signifies J/ψ or $\psi(3686)$, ξ denotes the polar angle and azimuthal angle of the particle in its final state,

T_k ($k = 0, 1, \dots, 6$) is a set of seven angular functions, and α_0 ($\bar{\alpha}_0$) is the decay asymmetry parameter of $\Sigma^+ \rightarrow p \pi^0$ ($\bar{\Sigma}^- \rightarrow \bar{p} \pi^0$). The explicit dependence on the decay asymmetry parameters α_0 and $\bar{\alpha}_0$ enables their simultaneous extraction. Equation (1) consists of three main contributions: one unpolarized part (involving T_0 and T_5) describing the scattering angular distribution, one part (with T_1 , T_2 , and T_6) describing the spin correlation between the Σ^+ and the $\bar{\Sigma}^-$, and, finally, the spin polarization of the Σ^+ and $\bar{\Sigma}^-$ (with T_3 and T_4 , respectively). The spin-correlated part and the spin-polarization part are governed by the psionic form-factor phase $\Delta\Phi$ and depend on the Σ^+ scattering angle via

$$\mathbf{P}_h(\cos \theta_{\Sigma^+}) = \frac{\sqrt{1 - \alpha_\Psi^2} \sin(\Delta\Phi) \cos \theta_{\Sigma^+} \sin \theta_{\Sigma^+}}{1 + \alpha_\Psi \cos^2 \theta_{\Sigma^+}}, \quad (2)$$

where the polarization direction is perpendicular to the $\Sigma^+ \bar{\Sigma}^-$ production plane. A nonzero phase $\Delta\Phi$ means that the Σ^+ and $\bar{\Sigma}^-$ hyperons are polarized even if the initial state is unpolarized.

To apply the formalism to data, the full reaction $e^+ e^- \rightarrow \Psi \rightarrow \Sigma^+ \bar{\Sigma}^- \rightarrow p \bar{p} \pi^0 \pi^0 \rightarrow p \bar{p} \gamma \gamma \gamma \gamma$ is selected based on the datasets collected with the BESIII detector. Although the final state formally contains four photons, only one π^0 is fully reconstructed from two photons, while the π^0 from the $\bar{\Sigma}^-$ decay is inferred through a kinematic fit. Details about the design and performance of the BESIII detector at the BEPCII collider are given in Ref. [37]. Selected event candidates must have two well-reconstructed charged tracks with net zero charge. Charged tracks detected in the multilayer drift chamber (MDC) are required to be within a polar angle (θ) range of $|\cos \theta| < 0.93$, where θ is defined with respect to the z axis, which is the symmetry axis of the MDC. For each charged track, the distance of closest approach to the interaction point (IP) must be less than 10 cm along the z axis and less than 2 cm in the transverse plane. Particle identification (PID) for charged tracks combines measurements of the specific ionization energy loss in the MDC (dE/dx) and the flight time in the time of flight to form likelihoods $\mathcal{L}(h)$ ($h = p, K, \pi$) for each hadron h hypothesis. Tracks are identified as protons or antiprotons when these hypotheses have the greatest likelihood [$\mathcal{L}(p) > \mathcal{L}(K)$ and $\mathcal{L}(p) > \mathcal{L}(\pi)$]. The distance of closest approaches of the proton and antiproton tracks to the IP is required to be larger than 0.34 cm, a criterion optimized to suppress background events that do not originate from Σ decays.

Photon candidates are identified using showers in the electromagnetic calorimeter (EMC). The deposited energy of each shower must be more than 25 MeV in the barrel region ($|\cos \theta| < 0.80$) and more than 50 MeV in the end-cap region ($0.86 < |\cos \theta| < 0.92$). To exclude showers originating from the charged tracks, the opening angle subtended by

the EMC shower and the position of the closest charged track at the EMC must be greater than 10° as measured from the IP. To suppress electronic noise and showers unrelated to the signal event, the difference between the EMC time and the event start time is required to be within $[0, 700]$ ns. To identify the π^0 candidates, the invariant mass $M_{\gamma\gamma}$ of the two photons has to satisfy $0.115 < M_{\gamma\gamma} < 0.150$ GeV/ c^2 . In addition, a one-constraint (1C) kinematic fit is performed to constrain $M_{\gamma\gamma}$ to the known π^0 mass [38], and only candidates with $\chi^2_{1C} < 200$ are retained. At least one π^0 candidate is selected per event. To further suppress background, a two-constraint (2C) kinematic fit is performed to the decay $\Psi \rightarrow p\pi^0\bar{p}\pi^0$, enforcing four-momentum conservation and applying a mass constraint on the π^0 from the Σ^+ decay. The π^0 from the $\bar{\Sigma}^-$ is not directly reconstructed. Instead, its three-momenta are treated as free variables and determined through the 2C kinematic fit. This approach reduces the background contamination produced by antiproton annihilation in the EMC and improves the selection efficiency. If there is more than one π^0 candidate, the one with the minimum χ^2_{2C} is selected. Events with $\chi^2_{2C} < 30$ are retained as signal candidates.

The inclusive Monte Carlo (MC) samples of 1.0×10^{10} J/ψ events and 2.7×10^9 $\psi(3686)$ events are used to investigate possible sources of contamination. MC events passing the event selection are examined with TopoAna, a generic event-type analysis tool [39]. All particle decays are modeled with EvtGen [40] using branching fractions either taken from the Particle Data Group [38], when available, or otherwise estimated by MC simulations based on Lundcharm [41]. The main peaking background contributions are $\Psi \rightarrow \gamma\Sigma^+\bar{\Sigma}^-$ and $\Psi \rightarrow \gamma\eta_c$ ($\eta_c \rightarrow \Sigma^+\bar{\Sigma}^-$), with fractions estimated to be 0.1%. The main sources of nonpeaking background are the decays $\Psi \rightarrow \Delta^+\bar{\Delta}^- \rightarrow p\pi^0\bar{p}\pi^0$ and $\Psi \rightarrow p\pi^0\bar{p}\pi^0$, which contribute 0.9% and 0.7% of the total data samples for J/ψ and $\psi(3686)$, respectively. Given the low level of peaking background, the sideband method is suitable for performing the background subtraction. Figure 2 shows the distribution of the invariant masses $M_{\bar{p}\pi^0}$ versus $M_{p\pi^0}$ from $\psi(3686)$ decays. The signal region in the green rectangle is defined as $1.167 < M_{\bar{p}\pi^0} < 1.212$ GeV/ c^2 and $1.172 < M_{p\pi^0} < 1.200$ GeV/ c^2 . To determine the background contributions in the signal region, the sideband regions in the red rectangles are defined as $1.118 < M_{\bar{p}\pi^0} < 1.140$ GeV/ c^2 , $1.240 < M_{\bar{p}\pi^0} < 1.262$ GeV/ c^2 , and $1.172 < M_{p\pi^0} < 1.200$ GeV/ c^2 . The mass windows are approximately $\pm 3\sigma$ away from the known $\bar{\Sigma}^-$ mass [38], with σ being the $M_{\bar{p}\pi^0}$ mass resolution. The background yields are estimated to be $f \times B$, where B is the total number of events in the two sidebands considered and $f = 1.06$ denotes the ratio of the background events between the signal and sideband regions determined by fitting the

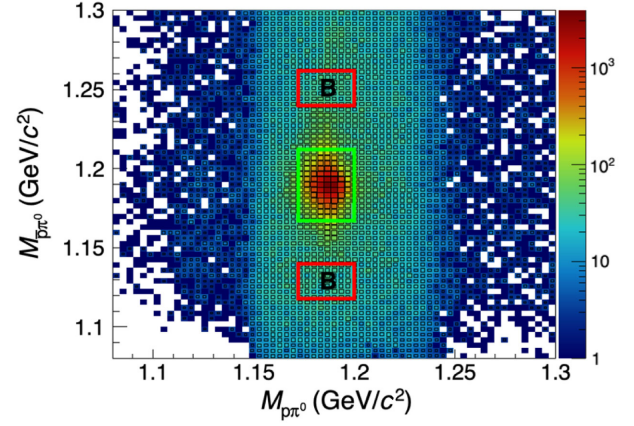


FIG. 2. Distribution of $M_{\bar{p}\pi^0}$ versus $M_{p\pi^0}$ for the $\psi(3686)$ data sample. The green box denotes the signal region, and the red ones indicate the sideband regions used for background estimation. The total number of events in the two sideband regions is denoted by B .

invariant mass distribution of \bar{p} and π^0 . The same procedure is applied to J/ψ sample, yielding also $f = 1.06$. After background subtraction, the signal event yields are 1011678 ± 1398 for J/ψ and 53293 ± 299 for $\psi(3686)$ decays.

An unbinned maximum likelihood fit is performed with the five-dimensional angular distribution described in Eq. (1). The fit is applied simultaneously to the J/ψ and $\psi(3686)$ datasets, with six free parameters $\alpha_{J/\psi}$, $\alpha_{\psi(3686)}$, $\Delta\Phi_{J/\psi}$, $\Delta\Phi_{\psi(3686)}$, α_0 , and $\bar{\alpha}_0$. Reconstruction efficiencies are incorporated in a model-independent way following the method outlined in Ref. [20], and the background contribution is included with the scale factor f . The numerical fit results are summarized in Table I. The correlation coefficient matrix of the fitted parameters is shown in Supplemental Material [42]. The CP asymmetry A_{CP} is determined to be $-0.0118 \pm 0.0083 \pm 0.0028$, consistent with CP conservation and representing the most precise measurement of this quantity in the hyperon sector. Under

TABLE I. Summary of fitted and derived parameters from the joint angular analysis of $\Psi \rightarrow \Sigma^+\bar{\Sigma}^- \rightarrow p\pi^0\bar{p}\pi^0$. The first uncertainty is statistical, and the second is systematic. The results are compared with previous BESIII measurements [22].

Parameter	This Letter	Previous result [22]
$\alpha_{J/\psi}$	$-0.5047 \pm 0.0018 \pm 0.0010$	$-0.508 \pm 0.006 \pm 0.004$
$\Delta\Phi_{J/\psi}$	$-0.2744 \pm 0.0033 \pm 0.0010$	$-0.270 \pm 0.012 \pm 0.009$
α_0	$-0.975 \pm 0.011 \pm 0.002$	$-0.998 \pm 0.037 \pm 0.009$
$\bar{\alpha}_0$	$0.999 \pm 0.011 \pm 0.004$	$0.990 \pm 0.037 \pm 0.011$
$\alpha_{\psi(3686)}$	$0.7133 \pm 0.0094 \pm 0.0065$	$0.682 \pm 0.030 \pm 0.011$
$\Delta\Phi_{\psi(3686)}$	$0.427 \pm 0.022 \pm 0.003$	$0.379 \pm 0.070 \pm 0.014$
$\langle\alpha_0\rangle$	$-0.9869 \pm 0.0011 \pm 0.0016$	$-0.994 \pm 0.004 \pm 0.002$
A_{CP}	$-0.0118 \pm 0.0083 \pm 0.0028$	$0.004 \pm 0.037 \pm 0.010$

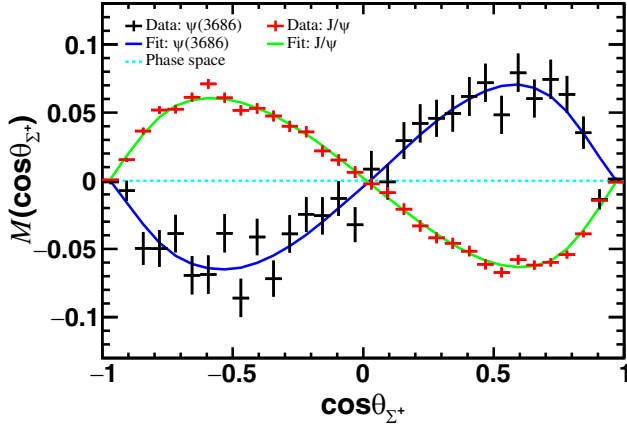


FIG. 3. The moment $M(\cos\theta_{\Sigma^+})$ for $\Psi \rightarrow \Sigma^+\bar{\Sigma}^- \rightarrow p\pi^0\bar{p}\pi^0$. Data points with error bars correspond to $\psi(3686)$ (black) and J/ψ (red) decays. Solid curves show the fit results based on the functional form $M(\cos\theta_{\Sigma^+}) \propto \sqrt{1-\alpha_\Psi^2}\langle\alpha_0\rangle\sin\Delta\Phi\sin\theta_{\Sigma^+}\cos\theta_{\Sigma^+}$, while the dashed cyan line is the expectation of an unpolarized phase space distribution.

the assumption of CP conservation, $\bar{\alpha}_0$ is replaced with $-\alpha_0$ in the fit. The average decay asymmetry parameter $\langle\alpha_0\rangle$ is fitted to be $-0.9869 \pm 0.0011 \pm 0.0016$, which represents the most precise determination of a decay asymmetry parameter in the baryon system. The relative phases between the Ψ electric and magnetic form factors are found to be $\Delta\Phi_{J/\psi} = -0.2744 \pm 0.0033 \pm 0.0010$ rad and $\Delta\Phi_{\psi(3686)} = 0.427 \pm 0.022 \pm 0.003$ rad, respectively. This sign difference indicates that the spins of the Σ^+ are aligned in opposite directions when produced via J/ψ decay compared to $\psi(3686)$ decay. This behavior was observed with limited statistics in earlier BESIII studies [21,22] and is now confirmed with significantly improved precision. The similar behavior was also observed in Σ^0 pair production [43]. To visualize the polarization, we define a polarization estimator $M(\cos\theta_{\Sigma^+})$ based on the helicity angles of the final-state proton and antiproton:

$$M(\cos\theta_{\Sigma^+}) = \frac{m}{N} \sum_i^{N(\cos\theta_{\Sigma^+})} (\sin\theta_p^i \sin\phi_p^i - \sin\theta_{\bar{p}}^i \sin\phi_{\bar{p}}^i), \quad (3)$$

where $m = 32$ is the number of bins, N is the total number of events, and $N(\cos\theta_{\Sigma^+})$ is the number of events in the $\cos\theta_{\Sigma^+}$ bin. Figure 3 shows the Σ^+ polarization distributions, clearly demonstrating the opposite polarization directions in J/ψ and $\psi(3686)$ decays.

To further investigate the difference between J/ψ and $\psi(3686)$ decays, the quantity $R(\cos\theta_{\Sigma^+})$ is defined as the ratio of the polarization values (\mathbf{P}_h) between $J/\psi \rightarrow \Sigma^+\bar{\Sigma}^-$ and $\psi(3686) \rightarrow \Sigma^+\bar{\Sigma}^-$ in each bin of $\cos\theta_{\Sigma^+}$. In this way, the model dependence of $\cos\theta_{\Sigma^+}$ is not introduced when extracting the polarization values. In Fig. 4, $R(\cos\theta_{\Sigma^+})$ is shown as a function of the Σ^+ scattering angle. $R(\cos\theta_{\Sigma^+})$

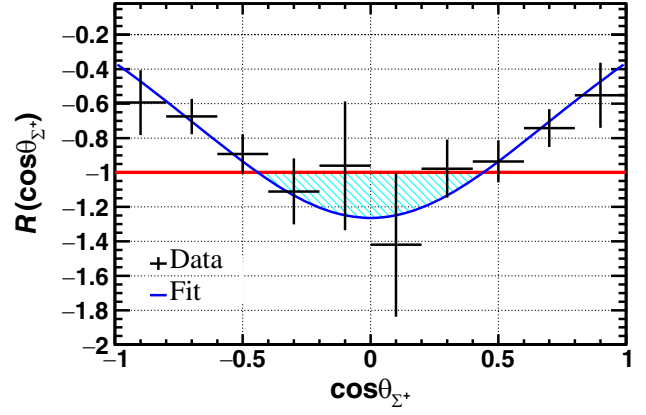


FIG. 4. Polarization ratio between J/ψ and $\psi(3686)$ decays as a function of the Σ^+ scattering angle. The black dots with error bars are the real data, and the blue solid line is the fitting results. The horizontal red line at -1 represents exact polarization reversal. The shaded area (perpendicular to the electron beam direction) indicates the enhanced polarization observed in $\psi(3686)$ compared to J/ψ decays.

is negative over the full angular range, indicating that the polarizations are oriented in the opposite direction in each bin. Benefiting from the increased sample size, the angular dependence of the polarization ratio $R(\cos\theta_{\Sigma^+})$ between J/ψ and $\psi(3686)$ decays is determined with unprecedented precision. It is found that the magnitude of $R(\cos\theta_{\Sigma^+})$ is minimum near $\cos\theta_{\Sigma^+} = \pm 1$, which corresponds to Σ^+ hyperons moving parallel (+) or antiparallel (−) to the positron beam. The magnitude of $R(\cos\theta_{\Sigma^+})$ increases away from these forward and backward directions and reaches a maximum in the direction perpendicular to the beam axis.

To interpret the production dynamics, we adopt the covariant L - S scheme [44–46] developed in Ref. [47], in which the decay amplitude of the process $\Psi \rightarrow \Sigma^+\bar{\Sigma}^-$ is decomposed into S -wave and D -wave components. The amplitude is expressed as $A = g_S \Psi_\mu^{(1)} \epsilon^\mu + g_D e^{i\delta} \Psi_\mu^{(1)} \epsilon_\nu \tilde{t}^{(2)\mu\nu}$, where g_S and g_D are the S -wave and D -wave coupling constants, respectively, and δ is the relative phase. $\Psi_\mu^{(1)}$ is the spin wave function, and $\tilde{t}^{(2)\mu\nu}$ is the D -wave orbital angular momentum covariant tensors. Using this framework, we extract the ratio between the S -wave and D -wave coupling constants g_D/g_S , their relative phase δ , and the percentage of the S -wave contribution $\Gamma_S/\Gamma_{\text{Total}}$. More importantly, the effective interaction radius \bar{r}_{eff} can be determined by calculating the average orbital angular momentum (\vec{L}) and the relative momentum (\vec{p}), where $\vec{L} = \vec{r}_{\text{eff}} \times \vec{p}$. As shown in Table II, the difference in δ between $J/\psi \rightarrow \Sigma^+\bar{\Sigma}^-$ and $\psi(3686) \rightarrow \Sigma^+\bar{\Sigma}^-$ is approximately π . The effective interaction radius r_{eff} is nearly identical for both J/ψ and $\psi(3686)$ with a value of approximately 0.036 fm.

The systematic uncertainties associated with the extracted parameters are listed in Supplemental Material [42]. The total

TABLE II. The parameters for the process $\psi \rightarrow \Sigma^+ \bar{\Sigma}^-$ (from Ref. [47]), including the ratio of D -wave to S -wave coupling constants (g_D/g_S), the relative phase between the S wave and D wave (δ), the ratio of the S -wave partial width to the total width ($\Gamma_S/\Gamma_{\text{Total}}$), and the effective radius (r_{eff}). The first and second uncertainties represent statistical and systematic, respectively.

Mode	g_D/g_S (GeV^{-2})	δ (rad)	$\Gamma_S/\Gamma_{\text{Total}}$ (%)	r_{eff} (fm)
$J/\psi \rightarrow \Sigma^+ \bar{\Sigma}^-$	$0.1700 \pm 0.0011 \pm 0.0005$	$2.661 \pm 0.007 \pm 0.002$	$90.97 \pm 0.10 \pm 0.05$	$0.0359 \pm 0.0004 \pm 0.0002$
$\psi(3686) \rightarrow \Sigma^+ \bar{\Sigma}^-$	$0.1034 \pm 0.0023 \pm 0.0010$	$-0.335 \pm 0.023 \pm 0.006$	$87.0 \pm 0.5 \pm 0.2$	$0.0365 \pm 0.0014 \pm 0.0006$

uncertainty for each parameter is obtained by summing individual contributions in quadrature. The main sources of systematic uncertainty include reconstruction efficiency corrections, the kinematic fit, signal mass window, background subtraction, and the fitting procedure. The uncertainties from charged-particle tracking, PID, and π^0 reconstruction efficiencies are studied using the control samples $J/\psi \rightarrow p \bar{p} \pi^+ \pi^-$ and $J/\psi \rightarrow \Sigma^+ \bar{\Sigma}^- \rightarrow p \pi^0 \bar{p} \pi^0$. The correction factors represent the efficiency differences between the data and MC. They are derived from the control samples and used to reweight phase-space MC samples. The full analysis is repeated 100 times with varied correction factors sampled from Gaussian distributions. The standard deviation of the fitted parameters is taken as the associated systematic uncertainty. The uncertainty from the kinematic fit is estimated by varying the selection requirement of $\chi^2_{2C} \leq 30$ from 20 to 40. The resulting deviations from the nominal fit are taken as the corresponding uncertainties. The uncertainty due to the requirement of the signal mass window is determined by changing the window range in $1 \text{ MeV}/c^2$ steps within $4 \text{ MeV}/c^2$ range. Similarly, the uncertainty associated with the background subtraction is evaluated by varying the sideband window in $1 \text{ MeV}/c^2$ steps within $4 \text{ MeV}/c^2$ range. In both cases, the largest difference relative to the nominal result is taken as the systematic uncertainty. To evaluate the reliability of parameter estimation with the maximum likelihood fit, 100 MC samples are generated with EvtGen. These samples are produced with the angular distributions based on Eq. (1) and input parameters set to the values extracted from data. The differences between the input and output values are interpreted as systematic uncertainties due to the fitting method.

In summary, we report a stringent test of CP symmetry using the quantum-entangled $\Sigma^+ \bar{\Sigma}^-$ system, based on $1.0087 \times 10^{10} J/\psi$ events and $2.7124 \times 10^9 \psi(3686)$ events collected by the BESIII experiment. The CP asymmetry is measured to be $A_{CP} = -0.0118 \pm 0.0083 \pm 0.0028$, consistent with CP conservation and representing the most precise result in Σ sector. The average value $\langle \alpha_0 \rangle = -0.9869 \pm 0.0011 \pm 0.0016$ is the most precise measurement in all baryon decays and provides a crucial input for precise decay parameter measurements and CP violation searches in the charm and beauty baryon decays to Σ^+ . A detailed comparison of hyperon polarization with sign flip between J/ψ and $\psi(3686)$ decays is performed for the first time. The study of polarization ratios helps to eliminate

theoretical uncertainties, enabling a better understanding of the internal structure of hyperons, such as diquark models [48,49]. Furthermore, these results offer new insights into SU(3) flavor symmetry breaking and nonperturbative QCD dynamics [50–52]. The precision of the parameters related to Σ pair production is improved by factors of 3 for $\alpha_{\psi(3686)}$, $\alpha_{J/\psi}$, and $\Delta\Phi_{\psi(3686)}$ and by a factor of 4 for $\Delta\Phi_{J/\psi}$. Using these parameters, we achieve the most precise effective interaction radius r_{eff} for the Σ hyperon, which is crucial for searches of excited baryons.

Our measurements are expected to remain the benchmark for Σ^+ hyperons for the next decade, until results become available from future higher-luminosity machines [12,15,53]. While previous studies have focused primarily on Λ hyperons, this high-precision study of Σ hyperons opens a complementary perspective. Given that both Σ and Λ hyperons contain a single strange quark, a comparative analysis will be essential for future investigations into strong interaction mechanisms and baryon structure.

Acknowledgments—The BESIII Collaboration thanks the staff of BEPCII and the IHEP computing center for their strong support. This work is supported in part by National Key R&D Program of China under Contracts No. 2023YFA1606000, No. 2020YFA0406300, and No. 2020YFA0406400; National Natural Science Foundation of China (NSFC) under Contracts No. 12375070, No. 11635010, No. 11735014, No. 11935015, No. 11935016, No. 11935018, No. 12025502, No. 12035009, No. 12035013, No. 12061131003, No. 12192260, No. 12192261, No. 12192262, No. 12192263, No. 12192264, No. 12192265, No. 12221005, No. 12225509, No. 12235017, and No. 12361141819; the Chinese Academy of Sciences (CAS) Large-Scale Scientific Facility Program; Shanghai Leading Talent Program of Eastern Talent Plan under Contract No. JLH5913002; the CAS Center for Excellence in Particle Physics (CCEPP); Joint Large-Scale Scientific Facility Funds of the NSFC and CAS under Contract No. U1832207; CAS under Contract No. YSBR-101; 100 Talents Program of CAS; The Institute of Nuclear and Particle Physics (INPAC) and Shanghai Key Laboratory for Particle Physics and Cosmology; Agencia Nacional de Investigación y Desarrollo de Chile (ANID), Chile under Contract No. ANID PIA/APOYO AFB230003; German Research

Foundation DFG under Contract No. FOR5327; Istituto Nazionale di Fisica Nucleare, Italy; Knut and Alice Wallenberg Foundation under Contracts No. 2021.0174 and No. 2021.0299; Ministry of Development of Turkey under Contract No. DPT2006K-120470; National Research Foundation of Korea under Contract No. NRF-2022R1A2C1092335; National Science and Technology fund of Mongolia; National Science Research and Innovation Fund (NSRF) via the Program Management Unit for Human Resources & Institutional Development, Research and Innovation of Thailand under Contract No. B50G670107; Polish National Science Centre under Contract No. 2019/35/O/ST2/02907; Swedish Research Council under Contract No. 2019.04595; The Swedish Foundation for International Cooperation in Research and Higher Education under Contract No. CH2018-7756; and U.S. Department of Energy under Contract No. DE-FG02-05ER41374.

Data availability—The data that support the findings of this article are not publicly available upon publication because it is not technically feasible and/or the cost of preparing, depositing, and hosting the data would be prohibitive within the terms of this research project. The data are available from the authors upon reasonable request.

-
- [1] A. D. Sakharov, *Sov. Phys. Usp.* **34**, 392 (1991).
 - [2] N. Cabibbo, *Phys. Rev. Lett.* **10**, 531 (1963).
 - [3] M. Kobayashi and T. Maskawa, *Prog. Theor. Phys.* **49**, 652 (1973).
 - [4] J. H. Christenson, J. W. Cronin, V. L. Fitch, and R. Turlay, *Phys. Rev. Lett.* **13**, 138 (1964).
 - [5] A. Abashian *et al.* (Belle Collaboration), *Phys. Rev. Lett.* **86**, 2509 (2001).
 - [6] B. Aubert *et al.* (BABAR Collaboration), *Phys. Rev. Lett.* **86**, 2515 (2001).
 - [7] Y. Chao *et al.* (Belle Collaboration), *Phys. Rev. Lett.* **93**, 191802 (2004).
 - [8] B. Aubert *et al.* (BABAR Collaboration), *Phys. Rev. Lett.* **93**, 131801 (2004).
 - [9] R. Aaij *et al.* (LHCb Collaboration), *Phys. Rev. Lett.* **122**, 211803 (2019).
 - [10] M. E. Peskin, *Nature (London)* **419**, 24 (2002).
 - [11] J. Tandean, *Phys. Rev. D* **69**, 076008 (2004).
 - [12] N. Salone, P. Adlarson, V. Batzskaya, A. Kupsc, S. Leupold, and J. Tandean, *Phys. Rev. D* **105**, 116022 (2022).
 - [13] X. G. He, J. Tandean, and G. Valencia, *Sci. Bull.* **67**, 1840 (2022).
 - [14] X. G. He, H. Murayama, S. Pakvasa, and G. Valencia, *Phys. Rev. D* **61**, 071701(R) (2000).
 - [15] E. Goudzovski, D. Redigolo, K. Tobioka, J. Zupan, G. Alonso-Álvarez, D. S. M. Alves, S. Bansal, M. Bauer, J. Brod, V. Chobanova *et al.*, *Rep. Prog. Phys.* **86**, 016201 (2023).
 - [16] R. Aaij *et al.* (LHCb Collaboration), *Phys. Rev. Lett.* **134**, 101802 (2025).
 - [17] R. Aaij *et al.* (LHCb Collaboration), *Nature (London)* **643**, 1223 (2025).
 - [18] T. D. Lee, J. Steinberger, G. Feinberg, P. K. Kabir, and C. N. Yang, *Phys. Rev.* **106**, 1367 (1957).
 - [19] M. Ablikim *et al.* (BESIII Collaboration), *Nature (London)* **606**, 64 (2022).
 - [20] M. Ablikim *et al.* (BESIII Collaboration), *Phys. Rev. Lett.* **129**, 131801 (2022).
 - [21] M. Ablikim *et al.* (BESIII Collaboration), *Phys. Rev. Lett.* **131**, 191802 (2023).
 - [22] M. Ablikim *et al.* (BESIII Collaboration), *Phys. Rev. Lett.* **125**, 052004 (2020).
 - [23] J. F. Donoghue, X. G. He, and S. Pakvasa, *Phys. Rev. D* **34**, 833 (1986).
 - [24] J. Tandean and G. Valencia, *Phys. Rev. D* **67**, 056001 (2003).
 - [25] M. Ablikim *et al.* (BESIII Collaboration), *Chin. Phys. C* **41**, 013001 (2017).
 - [26] M. Ablikim *et al.* (BESIII Collaboration), *Chin. Phys. C* **42**, 023001 (2018).
 - [27] R. Baldini Ferroli, A. Mangoni, S. Pacetti, and K. Zhu, *Phys. Lett. B* **799**, 135041 (2019).
 - [28] S. Dobbs, K. K. Seth, A. Tomaradze, T. Xiao, and G. Bonvicini, *Phys. Rev. D* **96**, 092004 (2017).
 - [29] R. L. Jaffe and F. Wilczek, *Phys. Rev. Lett.* **91**, 232003 (2003).
 - [30] M. Ablikim *et al.* (BESIII Collaboration), *Chin. Phys. C* **48**, 093001 (2024).
 - [31] M. Ablikim *et al.* (BESIII Collaboration), *Chin. Phys. C* **46**, 074001 (2022).
 - [32] G. Fäldt and A. Kupsc, *Phys. Lett. B* **772**, 16 (2017).
 - [33] A. Z. Dubnickova, S. Dubnicka, and M. P. Rekalov, *Nuovo Cimento Soc. Ital. Fis.* **109A**, 241 (1996).
 - [34] G. I. Gakh and E. Tomasi-Gustafsson, *Nucl. Phys. A* **771**, 169 (2006).
 - [35] G. Fäldt, *Eur. Phys. J. A* **51**, 74 (2015).
 - [36] G. Fäldt, *Eur. Phys. J. A* **52**, 141 (2016).
 - [37] M. Ablikim *et al.* (BESIII Collaboration), *Nucl. Instrum. Methods Phys. Res., Sect. A* **614**, 345 (2010).
 - [38] S. Navas *et al.* (Particle Data Group), *Phys. Rev. D* **110**, 030001 (2024).
 - [39] X. Y. Zhou, S. X. Du, G. Li, and C. P. Shen, *Comput. Phys. Commun.* **258**, 107540 (2021).
 - [40] D. J. Lange, *Nucl. Instrum. Methods Phys. Res., Sect. A* **462**, 152 (2001); R. G. Ping, *Chin. Phys. C* **32**, 599 (2008).
 - [41] J. C. Chen, G. S. Huang, X. R. Qi, D. H. Zhang, and Y. S. Zhu, *Phys. Rev. D* **62**, 034003 (2000); R. L. Yang, R. G. Ping, and H. Chen, *Chin. Phys. Lett.* **31**, 061301 (2014).
 - [42] See Supplemental Material at <http://link.aps.org/supplemental/10.1103/ysd5-s2gn>, which includes additional information about the invariant mass distributions of $M_{\pi\pi^0}$ and $M_{\bar{\pi}\pi^0}$, correlations between the fitted parameters, and a detailed source of the systematic uncertainties.
 - [43] M. Ablikim *et al.* (BESIII Collaboration), *Phys. Rev. Lett.* **133**, 101902 (2024).
 - [44] B. S. Zou and F. Hussain, *Phys. Rev. C* **67**, 015204 (2003).
 - [45] S. Dulat, J. J. Wu, and B. S. Zou, *Phys. Rev. D* **83**, 094032 (2011).
 - [46] S. U. Chung, *Phys. Rev. D* **48**, 1225 (1993).
 - [47] S. M. Wu, J. J. Wu, and B. S. Zou, *Phys. Rev. D* **104**, 054018 (2021).

- [48] Y. Yang, Z. Lu, and I. Schmidt, *Phys. Rev. D* **96**, 034010 (2017).
- [49] Y. Guan *et al.* (Belle Collaboration), *Phys. Rev. Lett.* **122**, 042001 (2019).
- [50] J. M. Bickerton, R. Horsley, Y. Nakamura, H. Perl, D. Pleiter, P. E. L. Rakow, G. Schierholz, H. Stüben, R. D. Young, and J. M. Zanotti, *Phys. Rev. D* **100**, 114516 (2019).
- [51] B. Borasoy and B. R. Holstein, *Eur. Phys. J. C* **6**, 85 (1999).
- [52] A. Le Yaoouanc, O. Pene, J. C. Raynal, and L. Oliver, *Nucl. Phys. B* **149**, 321 (1979).
- [53] M. Achasov, X. C. Ai, R. Aliberti, L. P. An, Q. An, X. Z. Bai, Y. Bai, O. Bakina, A. Barnyakov, V. Blinov *et al.*, *Front. Phys. (Beijing)* **19**, 14701 (2024).
-
- M. Ablikim,¹ M. N. Achasov,^{4,c} P. Adlarson,⁷⁶ X. C. Ai,⁸¹ R. Aliberti,³⁵ A. Amoroso,^{75a,75c} Q. An,^{72,58,a} Y. Bai,⁵⁷ O. Bakina,³⁶ Y. Ban,^{46,h} H.-R. Bao,⁶⁴ V. Batozskaya,^{1,44} K. Begzsuren,³² N. Berger,³⁵ M. Berlowski,⁴⁴ M. Bertani,^{28a} D. Bettoni,^{29a} F. Bianchi,^{75a,75c} E. Bianco,^{75a,75c} A. Bortone,^{75a,75c} I. Boyko,³⁶ R. A. Briere,⁵ A. Brueggemann,⁶⁹ H. Cai,⁷⁷ M. H. Cai,^{38,k,l} X. Cai,^{1,58} A. Calcaterra,^{28a} G. F. Cao,^{1,64} N. Cao,^{1,64} S. A. Cetin,^{62a} X. Y. Chai,^{46,h} J. F. Chang,^{1,58} G. R. Che,⁴³ Y. Z. Che,^{1,58,64} G. Chelkov,^{36,b} C. Chen,⁴³ C. H. Chen,⁹ Chao Chen,⁵⁵ G. Chen,¹ H. S. Chen,^{1,64} H. Y. Chen,²⁰ M. L. Chen,^{1,58,64} S. J. Chen,⁴² S. L. Chen,⁴⁵ S. M. Chen,⁶¹ T. Chen,^{1,64} X. R. Chen,^{31,64} X. T. Chen,^{1,64} Y. B. Chen,^{1,58} Y. Q. Chen,³⁴ Z. J. Chen,^{25,i} Z. K. Chen,⁵⁹ S. K. Choi,¹⁰ X. Chu,^{12,g} G. Cibinetto,^{29a} F. Cossio,^{75c} J. J. Cui,⁵⁰ H. L. Dai,^{1,58} J. P. Dai,⁷⁹ A. Dbeyssi,¹⁸ R. E. de Boer,³ D. Dedovich,³⁶ C. Q. Deng,⁷³ Z. Y. Deng,¹ A. Denig,³⁵ I. Denysenko,³⁶ M. Destefanis,^{75a,75c} F. De Mori,^{75a,75c} B. Ding,^{67,1} X. X. Ding,^{46,h} Y. Ding,³⁴ Y. Ding,⁴⁰ Y. X. Ding,³⁰ J. Dong,^{1,58} L. Y. Dong,^{1,64} M. Y. Dong,^{1,58,64} X. Dong,⁷⁷ M. C. Du,¹ S. X. Du,⁸¹ Y. Y. Duan,⁵⁵ Z. H. Duan,⁴² P. Egorov,^{36,b} G. F. Fan,⁴² J. J. Fan,¹⁹ Y. H. Fan,⁴⁵ J. Fang,⁵⁹ J. Fang,^{1,58} S. S. Fang,^{1,64} W. X. Fang,¹ Y. Q. Fang,^{1,58} R. Farinelli,^{29a} L. Fava,^{75b,75c} F. Feldbauer,³ G. Felici,^{28a} C. Q. Feng,^{72,58} J. H. Feng,⁵⁹ Y. T. Feng,^{72,58} M. Fritsch,³ C. D. Fu,¹ J. L. Fu,⁶⁴ Y. W. Fu,^{1,64} H. Gao,⁶⁴ X. B. Gao,⁴¹ Y. N. Gao,^{46,h} Y. N. Gao,¹⁹ Y. Y. Gao,³⁰ Yang Gao,^{72,58} S. Garbolino,^{75c} I. Garzia,^{29a,29b} P. T. Ge,¹⁹ Z. W. Ge,⁴² C. Geng,⁵⁹ E. M. Gersabeck,⁶⁸ A. Gilman,⁷⁰ K. Goetzen,¹³ J. D. Gong,³⁴ L. Gong,⁴⁰ W. X. Gong,^{1,58} W. Gradl,³⁵ S. Gramigna,^{29a,29b} M. Greco,^{75a,75c} M. H. Gu,^{1,58} Y. T. Gu,¹⁵ C. Y. Guan,^{1,64} A. Q. Guo,³¹ L. B. Guo,⁴¹ M. J. Guo,⁵⁰ R. P. Guo,⁴⁹ Y. P. Guo,^{12,g} A. Guskov,^{36,b} J. Gutierrez,²⁷ K. L. Han,⁶⁴ T. T. Han,¹ F. Hanisch,³ K. D. Hao,^{72,58} X. Q. Hao,¹⁹ F. A. Harris,⁶⁶ K. K. He,⁵⁵ K. L. He,^{1,64} F. H. Heinsius,³ C. H. Heinz,³⁵ Y. K. Heng,^{1,58,64} C. Herold,⁶⁰ T. Holtmann,³ P. C. Hong,³⁴ G. Y. Hou,^{1,64} X. T. Hou,^{1,64} Y. R. Hou,⁶⁴ Z. L. Hou,¹ B. Y. Hu,⁵⁹ H. M. Hu,^{1,64} J. F. Hu,^{56,j} Q. P. Hu,^{72,58} S. L. Hu,^{12,g} T. Hu,^{1,58,64} Y. Hu,¹ Z. M. Hu,⁵⁹ G. S. Huang,^{72,58} K. X. Huang,⁵⁹ L. Q. Huang,^{31,64} P. Huang,⁴² X. T. Huang,⁵⁰ Y. P. Huang,¹ Y. S. Huang,⁵⁹ T. Hussain,⁷⁴ N. Hüsken,³⁵ N. in der Wiesche,⁶⁹ J. Jackson,²⁷ S. Janchiv,³² Q. Ji,¹ Q. P. Ji,¹⁹ W. Ji,^{1,64} X. B. Ji,^{1,64} X. L. Ji,^{1,58} Y. Y. Ji,⁵⁰ Z. K. Jia,^{72,58} D. Jiang,^{1,64} H. B. Jiang,⁷⁷ P. C. Jiang,^{46,h} S. J. Jiang,⁹ T. J. Jiang,¹⁶ X. S. Jiang,^{1,58,64} Y. Jiang,⁶⁴ J. B. Jiao,⁵⁰ J. K. Jiao,³⁴ Z. Jiao,²³ S. Jin,⁴² Y. Jin,⁶⁷ M. Q. Jing,^{1,64} X. M. Jing,⁶⁴ T. Johansson,⁷⁶ S. Kabana,³³ N. Kalantar-Nayestanaki,⁶⁵ X. L. Kang,⁹ X. S. Kang,⁴⁰ M. Kavatsyuk,⁶⁵ B. C. Ke,⁸¹ V. Khachatryan,²⁷ A. Khoukaz,⁶⁹ R. Kiuchi,¹ O. B. Kolcu,^{62a} B. Kopf,³ M. Kuessner,³ X. Kui,^{1,64} N. Kumar,²⁶ A. Kupsc,^{44,76} W. Kühn,³⁷ Q. Lan,⁷³ W. N. Lan,¹⁹ T. T. Lei,^{72,58} M. Lellmann,³⁵ T. Lenz,³⁵ C. Li,⁴³ C. Li,⁴⁷ C. H. Li,³⁹ C. K. Li,²⁰ Cheng Li,^{72,58} D. M. Li,⁸¹ F. Li,^{1,58} G. Li,¹ H. B. Li,^{1,64} H. J. Li,¹⁹ H. N. Li,^{56,j} Hui Li,⁴³ J. R. Li,⁶¹ J. S. Li,⁵⁹ K. Li,¹ K. L. Li,^{38,k,l} K. L. Li,¹⁹ L. J. Li,^{1,64} Lei Li,⁴⁸ M. H. Li,⁴³ M. R. Li,^{1,64} P. L. Li,⁶⁴ P. R. Li,^{38,k,l} Q. M. Li,^{1,64} Q. X. Li,⁵⁰ R. Li,^{17,31} T. Li,⁵⁰ T. Y. Li,⁴³ W. D. Li,^{1,64} W. G. Li,^{1,a} X. Li,^{1,64} X. H. Li,^{72,58} X. L. Li,⁵⁰ X. Y. Li,^{1,8} X. Z. Li,⁵⁹ Y. Li,¹⁹ Y. G. Li,^{46,h} Y. P. Li,³⁴ Z. J. Li,⁵⁹ Z. Y. Li,⁷⁹ C. Liang,⁴² H. Liang,^{72,58} Y. F. Liang,⁵⁴ Y. T. Liang,^{31,64} G. R. Liao,¹⁴ L. B. Liao,⁵⁹ M. H. Liao,⁵⁹ Y. P. Liao,^{1,64} J. Libby,²⁶ A. Limphirat,⁶⁰ C. C. Lin,⁵⁵ C. X. Lin,⁶⁴ D. X. Lin,^{31,64} L. Q. Lin,³⁹ T. Lin,¹ B. J. Liu,¹ B. X. Liu,⁷⁷ C. Liu,³⁴ C. X. Liu,¹ F. Liu,¹ F. H. Liu,⁵³ Feng Liu,⁶ G. M. Liu,^{56,j} H. Liu,^{38,k,l} H. B. Liu,¹⁵ H. H. Liu,¹ H. M. Liu,^{1,64} Huihui Liu,²¹ J. B. Liu,^{72,58} J. J. Liu,²⁰ K. Liu,^{38,k,l} K. Liu,⁷³ K. Y. Liu,⁴⁰ Ke Liu,²² L. Liu,^{72,58} L. C. Liu,⁴³ Lu Liu,⁴³ P. L. Liu,¹ Q. Liu,⁶⁴ S. B. Liu,^{72,58} T. Liu,^{12,g} W. K. Liu,⁴³ W. M. Liu,^{72,58} W. T. Liu,³⁹ X. Liu,^{38,k,l} X. Liu,³⁹ X. Y. Liu,⁷⁷ Y. Liu,^{38,k,l} Y. Liu,⁸¹ Y. Liu,⁸¹ Y. B. Liu,⁴³ Z. A. Liu,^{1,58,64} Z. D. Liu,⁹ Z. Q. Liu,⁵⁰ X. C. Lou,^{1,58,64} F. X. Lu,⁵⁹ H. J. Lu,²³ J. G. Lu,^{1,58} Y. Lu,⁷ Y. H. Lu,^{1,64} Y. P. Lu,^{1,58} Z. H. Lu,^{1,64} C. L. Luo,⁴¹ J. R. Luo,⁵⁹ J. S. Luo,^{1,64} M. X. Luo,⁸⁰ T. Luo,^{12,g} X. L. Luo,^{1,58} Z. Y. Lv,²² X. R. Lyu,^{64,p} Y. F. Lyu,⁴³ Y. H. Lyu,⁸¹ F. C. Ma,⁴⁰ H. Ma,⁷⁹ H. L. Ma,¹ J. L. Ma,^{1,64} L. L. Ma,⁵⁰ L. R. Ma,⁶⁷ Q. M. Ma,¹ R. Q. Ma,^{1,64} R. Y. Ma,¹⁹ T. Ma,^{72,58} X. T. Ma,^{1,64} X. Y. Ma,^{1,58} Y. M. Ma,³¹ F. E. Maas,¹⁸ I. MacKay,⁷⁰ M. Maggiora,^{75a,75c} S. Malde,⁷⁰ Y. J. Mao,^{46,h} Z. P. Mao,¹ S. Marcello,^{75a,75c} F. M. Melendi,^{29a,29b} Y. H. Meng,⁶⁴ Z. X. Meng,⁶⁷ J. G. Messchendorp,^{13,65} G. Mezzadri,^{29a} H. Miao,^{1,64} T. J. Min,⁴² R. E. Mitchell,²⁷ X. H. Mo,^{1,58,64} B. Moses,²⁷ N. Yu. Muchnoi,^{4,c} J. Muskalla,³⁵ Y. Nefedov,³⁶ F. Nerling,^{18,e} L. S. Nie,²⁰ I. B. Nikolaev,^{4,c} Z. Ning,^{1,58} S. Nisar,^{11,m}

Q. L. Niu,^{38,k,l} W. D. Niu,^{12,g} S. L. Olsen,^{10,64} Q. Ouyang,^{1,58,64} S. Pacetti,^{28b,28c} X. Pan,⁵⁵ Y. Pan,⁵⁷ A. Pathak,¹⁰ Y. P. Pei,^{72,58}
 M. Pelizaeus,³ H. P. Peng,^{72,58} Y. Y. Peng,^{38,k,l} K. Peters,^{13,e} J. L. Ping,⁴¹ R. G. Ping,^{1,64} S. Plura,³⁵ V. Prasad,³³ F. Z. Qi,¹
 H. R. Qi,⁶¹ M. Qi,⁴² S. Qian,^{1,58} W. B. Qian,⁶⁴ C. F. Qiao,⁶⁴ J. H. Qiao,¹⁹ J. J. Qin,⁷³ J. L. Qin,⁵⁵ L. Q. Qin,¹⁴ L. Y. Qin,^{72,58}
 P. B. Qin,⁷³ X. P. Qin,^{12,g} X. S. Qin,⁵⁰ Z. H. Qin,^{1,58} J. F. Qiu,¹ Z. H. Qu,⁷³ C. F. Redmer,³⁵ A. Rivetti,^{75c} M. Rolo,^{75c}
 G. Rong,^{1,64} S. S. Rong,^{1,64} F. Rosini,^{28b,28c} Ch. Rosner,¹⁸ M. Q. Ruan,^{1,58} S. N. Ruan,⁴³ N. Salone,⁴⁴ A. Sarantsev,^{36,d}
 Y. Schelhaas,³⁵ K. Schoenning,⁷⁶ M. Scodeggio,^{29a} K. Y. Shan,^{12,g} W. Shan,²⁴ X. Y. Shan,^{72,58} Z. J. Shang,^{38,k,l}
 J. F. Shangguan,¹⁶ L. G. Shao,^{1,64} M. Shao,^{72,58} C. P. Shen,^{12,g} H. F. Shen,^{1,8} W. H. Shen,⁶⁴ X. Y. Shen,^{1,64} B. A. Shi,⁶⁴
 H. Shi,^{72,58} J. L. Shi,^{12,g} J. Y. Shi,¹ S. Y. Shi,⁷³ X. Shi,^{1,58} H. L. Song,^{72,58} J. J. Song,¹⁹ T. Z. Song,⁵⁹ W. M. Song,^{34,1}
 Y. X. Song,^{46,h,n} S. Sosio,^{75a,75c} S. Spataro,^{75a,75c} F. Stieler,³⁵ S. S. Su,⁴⁰ Y. J. Su,⁶⁴ G. B. Sun,⁷⁷ G. X. Sun,¹ H. Sun,⁶⁴
 H. K. Sun,¹ J. F. Sun,¹⁹ K. Sun,⁶¹ L. Sun,⁷⁷ S. S. Sun,^{1,64} T. Sun,^{51,f} Y. C. Sun,⁷⁷ Y. H. Sun,³⁰ Y. J. Sun,^{72,58} Y. Z. Sun,¹
 Z. Q. Sun,^{1,64} Z. T. Sun,⁵⁰ C. J. Tang,⁵⁴ G. Y. Tang,¹ J. Tang,⁵⁹ L. F. Tang,³⁹ M. Tang,^{72,58} Y. A. Tang,⁷⁷ L. Y. Tao,⁷³ M. Tat,⁷⁰
 J. X. Teng,^{72,58} J. Y. Tian,^{72,58} W. H. Tian,⁵⁹ Y. Tian,³¹ Z. F. Tian,⁷⁷ I. Uman,^{62b} B. Wang,⁵⁹ B. Wang,¹ Bo Wang,^{72,58}
 C. Wang,¹⁹ Cong Wang,²² D. Y. Wang,^{46,h} H. J. Wang,^{38,k,l} J. J. Wang,⁷⁷ K. Wang,^{1,58} L. L. Wang,¹ L. W. Wang,³⁴
 M. Wang,⁵⁰ M. Wang,^{72,58} N. Y. Wang,⁶⁴ S. Wang,^{12,g} T. Wang,^{12,g} T. J. Wang,⁴³ W. Wang,⁷³ W. Wang,⁵⁹ W. P. Wang,^{35,58,72,o}
 X. Wang,^{46,h} X. F. Wang,^{38,k,l} X. J. Wang,³⁹ X. L. Wang,^{12,g} X. N. Wang,¹ Y. Wang,⁶¹ Y. D. Wang,⁴⁵ Y. F. Wang,^{1,58,64}
 Y. H. Wang,^{38,k,l} Y. L. Wang,¹⁹ Y. N. Wang,⁷⁷ Y. Q. Wang,¹ Yaqian Wang,¹⁷ Yi Wang,⁶¹ Yuan Wang,^{17,31} Z. Wang,^{1,58}
 Z. L. Wang,⁷³ Z. L. Wang,² Z. Q. Wang,^{12,g} Z. Y. Wang,^{1,64} D. H. Wei,¹⁴ H. R. Wei,⁴³ F. Weidner,⁶⁹ S. P. Wen,¹ Y. R. Wen,³⁹
 U. Wiedner,³ G. Wilkinson,⁷⁰ M. Wolke,⁷⁶ C. Wu,³⁹ J. F. Wu,^{1,8} L. H. Wu,¹ L. J. Wu,^{1,64} Lianjie Wu,¹⁹ S. G. Wu,^{1,64}
 S. M. Wu,⁶⁴ X. Wu,^{12,g} X. H. Wu,³⁴ Y. J. Wu,³¹ Z. Wu,^{1,58} L. Xia,^{72,58} X. M. Xian,³⁹ B. H. Xiang,^{1,64} T. Xiang,^{46,h}
 D. Xiao,^{38,k,l} G. Y. Xiao,⁴² H. Xiao,⁷³ Y. L. Xiao,^{12,g} Z. J. Xiao,⁴¹ C. Xie,⁴² K. J. Xie,^{1,64} X. H. Xie,^{46,h} Y. Xie,⁵⁰ Y. G. Xie,^{1,58}
 Y. H. Xie,⁶ Z. P. Xie,^{72,58} T. Y. Xing,^{1,64} C. F. Xu,^{1,64} C. J. Xu,⁵⁹ G. F. Xu,¹ H. Y. Xu,² H. Y. Xu,^{67,2} M. Xu,^{72,58} Q. J. Xu,¹⁶
 Q. N. Xu,³⁰ W. L. Xu,⁶⁷ X. P. Xu,⁵⁵ Y. Xu,⁴⁰ Y. Xu,^{12,g} Y. C. Xu,⁷⁸ Z. S. Xu,⁶⁴ H. Y. Yan,³⁹ L. Yan,^{12,g} W. B. Yan,^{72,58}
 W. C. Yan,⁸¹ W. P. Yan,¹⁹ X. Q. Yan,^{1,64} H. J. Yang,^{51,f} H. L. Yang,³⁴ H. X. Yang,¹ J. H. Yang,⁴² R. J. Yang,¹⁹ T. Yang,¹
 Y. Yang,^{12,g} Y. F. Yang,⁴³ Y. H. Yang,⁴² Y. Q. Yang,⁹ Y. X. Yang,^{1,64} Y. Z. Yang,¹⁹ M. Ye,^{1,58} M. H. Ye,⁸ Junhao Yin,⁴³
 Z. Y. You,⁵⁹ B. X. Yu,^{1,58,64} C. X. Yu,⁴³ G. Yu,¹³ J. S. Yu,^{25,i} M. C. Yu,⁴⁰ T. Yu,⁷³ X. D. Yu,^{46,h} Y. C. Yu,⁸¹ C. Z. Yuan,^{1,64}
 H. Yuan,^{1,64} J. Yuan,⁴⁵ J. Yuan,³⁴ L. Yuan,² S. C. Yuan,^{1,64} Y. Yuan,^{1,64} Z. Y. Yuan,⁵⁹ C. X. Yue,³⁹ Ying Yue,¹⁹ A. A. Zafar,⁷⁴
 S. H. Zeng,⁶³ X. Zeng,^{12,g} Y. Zeng,^{25,i} Y. J. Zeng,^{1,64} Y. J. Zeng,⁵⁹ X. Y. Zhai,³⁴ Y. H. Zhan,⁵⁹ A. Q. Zhang,^{1,64}
 B. L. Zhang,^{1,64} B. X. Zhang,¹ D. H. Zhang,⁴³ G. Y. Zhang,¹⁹ G. Y. Zhang,^{1,64} H. Zhang,^{72,58} H. Zhang,⁸¹ H. C. Zhang,^{1,58,64}
 H. H. Zhang,⁵⁹ H. Q. Zhang,^{1,58,64} H. R. Zhang,^{72,58} H. Y. Zhang,^{1,58} J. Zhang,⁵⁹ J. Zhang,⁸¹ J. J. Zhang,⁵² J. L. Zhang,²⁰
 J. Q. Zhang,⁴¹ J. S. Zhang,^{12,g} J. W. Zhang,^{1,58,64} J. X. Zhang,^{38,k,l} J. Y. Zhang,¹ J. Z. Zhang,^{1,64} Jianyu Zhang,⁶⁴
 L. M. Zhang,⁶¹ Lei Zhang,⁴² N. Zhang,⁸¹ P. Zhang,^{1,64} Q. Zhang,¹⁹ Q. Y. Zhang,³⁴ R. Y. Zhang,^{38,k,l} S. H. Zhang,^{1,64}
 Shulei Zhang,^{25,i} X. M. Zhang,¹ X. Y. Zhang,⁴⁰ X. Y. Zhang,⁵⁰ Y. Zhang,⁷³ Y. Zhang,¹ Y. T. Zhang,⁸¹ Y. H. Zhang,^{1,58}
 Y. M. Zhang,³⁹ Z. D. Zhang,¹ Z. H. Zhang,¹ Z. L. Zhang,³⁴ Z. L. Zhang,⁵⁵ Z. X. Zhang,¹⁹ Z. Y. Zhang,⁴³ Z. Y. Zhang,⁷⁷
 Z. Z. Zhang,⁴⁵ Zh. Zh. Zhang,¹⁹ G. Zhao,¹ J. Y. Zhao,^{1,64} J. Z. Zhao,^{1,58} L. Zhao,¹ Lei Zhao,^{72,58} M. G. Zhao,⁴³ N. Zhao,⁷⁹
 R. P. Zhao,⁶⁴ S. J. Zhao,⁸¹ Y. B. Zhao,^{1,58} Y. L. Zhao,⁵⁵ Y. X. Zhao,^{31,64} Z. G. Zhao,^{72,58} A. Zhemchugov,^{36,b} B. Zheng,⁷³
 B. M. Zheng,³⁴ J. P. Zheng,^{1,58} W. J. Zheng,^{1,64} X. R. Zheng,¹⁹ Y. H. Zheng,^{64,p} B. Zhong,⁴¹ X. Zhong,⁵⁹ H. Zhou,^{35,50,o}
 J. Q. Zhou,³⁴ J. Y. Zhou,³⁴ S. Zhou,⁶ X. Zhou,⁷⁷ X. K. Zhou,⁶ X. R. Zhou,^{72,58} X. Y. Zhou,³⁹ Y. Z. Zhou,^{12,g} Z. C. Zhou,²⁰
 A. N. Zhu,⁶⁴ J. Zhu,⁴³ K. Zhu,¹ K. J. Zhu,^{1,58,64} K. S. Zhu,^{12,g} L. Zhu,³⁴ L. X. Zhu,⁶⁴ S. H. Zhu,⁷¹ T. J. Zhu,^{12,g} W. D. Zhu,^{12,g}
 W. D. Zhu,⁴¹ W. J. Zhu,¹ W. Z. Zhu,¹⁹ Y. C. Zhu,^{72,58} Z. A. Zhu,^{1,64} X. Y. Zhuang,⁴³ J. H. Zou,¹ and J. Zu^{72,58}

(BESIII Collaboration)

¹*Institute of High Energy Physics, Beijing 100049, People's Republic of China*
²*Beihang University, Beijing 100191, People's Republic of China*
³*Bochum Ruhr-University, D-44780 Bochum, Germany*
⁴*Budker Institute of Nuclear Physics SB RAS (BINP), Novosibirsk 630090, Russia*
⁵*Carnegie Mellon University, Pittsburgh, Pennsylvania 15213, USA*
⁶*Central China Normal University, Wuhan 430079, People's Republic of China*
⁷*Central South University, Changsha 410083, People's Republic of China*
⁸*China Center of Advanced Science and Technology, Beijing 100190, People's Republic of China*

- ⁹*China University of Geosciences, Wuhan 430074, People's Republic of China*
- ¹⁰*Chung-Ang University, Seoul, 06974, Republic of Korea*
- ¹¹*COMSATS University Islamabad, Lahore Campus, Defence Road, Off Raiwind Road, 54000 Lahore, Pakistan*
- ¹²*Fudan University, Shanghai 200433, People's Republic of China*
- ¹³*GSI Helmholtzcentre for Heavy Ion Research GmbH, D-64291 Darmstadt, Germany*
- ¹⁴*Guangxi Normal University, Guilin 541004, People's Republic of China*
- ¹⁵*Guangxi University, Nanning 530004, People's Republic of China*
- ¹⁶*Hangzhou Normal University, Hangzhou 310036, People's Republic of China*
- ¹⁷*Hebei University, Baoding 071002, People's Republic of China*
- ¹⁸*Helmholtz Institute Mainz, Staudinger Weg 18, D-55099 Mainz, Germany*
- ¹⁹*Henan Normal University, Xinxiang 453007, People's Republic of China*
- ²⁰*Henan University, Kaifeng 475004, People's Republic of China*
- ²¹*Henan University of Science and Technology, Luoyang 471003, People's Republic of China*
- ²²*Henan University of Technology, Zhengzhou 450001, People's Republic of China*
- ²³*Huangshan College, Huangshan 245000, People's Republic of China*
- ²⁴*Hunan Normal University, Changsha 410081, People's Republic of China*
- ²⁵*Hunan University, Changsha 410082, People's Republic of China*
- ²⁶*Indian Institute of Technology Madras, Chennai 600036, India*
- ²⁷*Indiana University, Bloomington, Indiana 47405, USA*
- ^{28a}*INFN Laboratori Nazionali di Frascati, INFN Laboratori Nazionali di Frascati, I-00044, Frascati, Italy*
- ^{28b}*INFN Sezione di Perugia, I-06100 Perugia, Italy*
- ^{28c}*University of Perugia, I-06100 Perugia, Italy*
- ^{29a}*INFN Sezione di Ferrara, INFN Sezione di Ferrara, I-44122 Ferrara, Italy*
- ^{29b}*University of Ferrara, I-44122 Ferrara, Italy*
- ³⁰*Inner Mongolia University, Hohhot 010021, People's Republic of China*
- ³¹*Institute of Modern Physics, Lanzhou 730000, People's Republic of China*
- ³²*Institute of Physics and Technology, Peace Avenue 54B, Ulaanbaatar 13330, Mongolia*
- ³³*Instituto de Alta Investigación, Universidad de Tarapacá, Casilla 7D, Arica 1000000, Chile*
- ³⁴*Jilin University, Changchun 130012, People's Republic of China*
- ³⁵*Johannes Gutenberg University of Mainz, Johann-Joachim-Becher-Weg 45, D-55099 Mainz, Germany*
- ³⁶*Joint Institute for Nuclear Research, 141980 Dubna, Moscow region, Russia*
- ³⁷*Justus-Liebig-Universität Giessen, II. Physikalisches Institut, Heinrich-Buff-Ring 16, D-35392 Giessen, Germany*
- ³⁸*Lanzhou University, Lanzhou 730000, People's Republic of China*
- ³⁹*Liaoning Normal University, Dalian 116029, People's Republic of China*
- ⁴⁰*Liaoning University, Shenyang 110036, People's Republic of China*
- ⁴¹*Nanjing Normal University, Nanjing 210023, People's Republic of China*
- ⁴²*Nanjing University, Nanjing 210093, People's Republic of China*
- ⁴³*Nankai University, Tianjin 300071, People's Republic of China*
- ⁴⁴*National Centre for Nuclear Research, Warsaw 02-093, Poland*
- ⁴⁵*North China Electric Power University, Beijing 102206, People's Republic of China*
- ⁴⁶*Peking University, Beijing 100871, People's Republic of China*
- ⁴⁷*Qufu Normal University, Qufu 273165, People's Republic of China*
- ⁴⁸*Renmin University of China, Beijing 100872, People's Republic of China*
- ⁴⁹*Shandong Normal University, Jinan 250014, People's Republic of China*
- ⁵⁰*Shandong University, Jinan 250100, People's Republic of China*
- ⁵¹*Shanghai Jiao Tong University, Shanghai 200240, People's Republic of China*
- ⁵²*Shanxi Normal University, Linfen 041004, People's Republic of China*
- ⁵³*Shanxi University, Taiyuan 030006, People's Republic of China*
- ⁵⁴*Sichuan University, Chengdu 610064, People's Republic of China*
- ⁵⁵*Soochow University, Suzhou 215006, People's Republic of China*
- ⁵⁶*South China Normal University, Guangzhou 510006, People's Republic of China*
- ⁵⁷*Southeast University, Nanjing 211100, People's Republic of China*
- ⁵⁸*State Key Laboratory of Particle Detection and Electronics, Beijing 100049, Hefei 230026, People's Republic of China*
- ⁵⁹*Sun Yat-Sen University, Guangzhou 510275, People's Republic of China*
- ⁶⁰*Suranaree University of Technology, University Avenue 111, Nakhon Ratchasima 30000, Thailand*
- ⁶¹*Tsinghua University, Beijing 100084, People's Republic of China*
- ^{62a}*Turkish Accelerator Center Particle Factory Group, Istinye University, 34010, Istanbul, Turkey*
- ^{62b}*Near East University, Nicosia, North Cyprus, 99138, Mersin 10, Turkey*
- ⁶³*University of Bristol, H H Wills Physics Laboratory, Tyndall Avenue, Bristol, BS8 1TL, United Kingdom*
- ⁶⁴*University of Chinese Academy of Sciences, Beijing 100049, People's Republic of China*

⁶⁵*University of Groningen, NL-9747 AA Groningen, The Netherlands*

⁶⁶*University of Hawaii, Honolulu, Hawaii 96822, USA*

⁶⁷*University of Jinan, Jinan 250022, People's Republic of China*

⁶⁸*University of Manchester, Oxford Road, Manchester, M13 9PL, United Kingdom*

⁶⁹*University of Muenster, Wilhelm-Klemm-Strasse 9, 48149 Muenster, Germany*

⁷⁰*University of Oxford, Keble Road, Oxford OX13RH, United Kingdom*

⁷¹*University of Science and Technology Liaoning, Anshan 114051, People's Republic of China*

⁷²*University of Science and Technology of China, Hefei 230026, People's Republic of China*

⁷³*University of South China, Hengyang 421001, People's Republic of China*

⁷⁴*University of the Punjab, Lahore-54590, Pakistan*

^{75a}*University of Turin and INFN, University of Turin, I-10125 Turin, Italy*

^{75b}*University of Eastern Piedmont, I-15121 Alessandria, Italy*

^{75c}*INFN, I-10125 Turin, Italy*

⁷⁶*Uppsala University, Box 516, SE-75120 Uppsala, Sweden*

⁷⁷*Wuhan University, Wuhan 430072, People's Republic of China*

⁷⁸*Yantai University, Yantai 264005, People's Republic of China*

⁷⁹*Yunnan University, Kunming 650500, People's Republic of China*

⁸⁰*Zhejiang University, Hangzhou 310027, People's Republic of China*

⁸¹*Zhengzhou University, Zhengzhou 450001, People's Republic of China*

^aDeceased.

^bAlso at the Moscow Institute of Physics and Technology, Moscow 141700, Russia.

^cAlso at the Novosibirsk State University, Novosibirsk, 630090, Russia.

^dAlso at the NRC "Kurchatov Institute," PNPI, 188300, Gatchina, Russia.

^eAlso at Goethe University Frankfurt, 60323 Frankfurt am Main, Germany.

^fAlso at Key Laboratory for Particle Physics, Astrophysics and Cosmology, Ministry of Education, Shanghai Key Laboratory for Particle Physics and Cosmology, Institute of Nuclear and Particle Physics, Shanghai 200240, People's Republic of China.

^gAlso at Key Laboratory of Nuclear Physics and Ion-beam Application (MOE) and Institute of Modern Physics, Fudan University, Shanghai 200443, People's Republic of China.

^hAlso at State Key Laboratory of Nuclear Physics and Technology, Peking University, Beijing 100871, People's Republic of China.

ⁱAlso at School of Physics and Electronics, Hunan University, Changsha 410082, China.

^jAlso at Guangdong Provincial Key Laboratory of Nuclear Science, Institute of Quantum Matter, South China Normal University, Guangzhou 510006, China.

^kAlso at MOE Frontiers Science Center for Rare Isotopes, Lanzhou University, Lanzhou 730000, People's Republic of China.

^lAlso at Lanzhou Center for Theoretical Physics, Lanzhou University, Lanzhou 730000, People's Republic of China.

^mAlso at the Department of Mathematical Sciences, IBA, Karachi 75270, Pakistan.

ⁿAlso at Ecole Polytechnique Federale de Lausanne (EPFL), CH-1015 Lausanne, Switzerland.

^oAlso at Helmholtz Institute Mainz, Staudinger Weg 18, D-55099 Mainz, Germany.

^pAlso at Hangzhou Institute for Advanced Study, University of Chinese Academy of Sciences, Hangzhou 310024, China.